

Magmatic history of Towada volcano: Part 1 - Petrological characteristics of the caldera-stage pyroclastic deposits

*Yuki Sato¹, Yoshimi Hiroi¹, Tsuyoshi MIYAMOTO²

1. Regulatory Standard and Research Department, Secretariat of Nuclear Regulation Authority (S/NRA/R), 2. Center for Northeast Asian Studies, Tohoku University

Eruptive history of Towada volcano, located northeast of Japan, has been categorized as eruptive episode A, eruptive episode B, eruptive episode C, etc., (hereafter, referred to as ep. A, ep. B, ep. C, etc.) in descending order of eruption age (Hayakawa, 1985). Large-scale eruptions accompanied by caldera subsidence occurred in ep. Q (61 ka; Horiuchi et al., 2017), ep. N (36 ka; Koiwa et al., 2007), and ep. L (15.5 ka; Ito et al., 2017). Hunter and Blake (1995) interpreted the period from ep. Q to ep. L when caldera eruptions occurred frequently as the caldera stage (61 ka to 15.5 ka), and similarly periods before and after this as the pre-caldera stage (200 ka to 61 ka) and the post-caldera stage (15.5 ka to present), respectively.

Magma compositions at Towada volcano vary from basaltic andesite to rhyolite throughout its eruptive history. Hunter and Blake (1995) argued that the various magma compositions identified from the caldera stage can be explained by assimilation and fractional crystallization (AFC) of one parental magma. However, the temporal variation in magma compositions along with the progression of volcanic activity has not been thoroughly addressed. Consideration of the temporal and spatial evolution of the magma plumbing system based on its eruptive history is important for constraining specific time scales of long-term and short-term processes associated with large-scale eruptions. In this study, we determined whole rock major and trace element compositions of pumices of two caldera eruptions (ep. N and ep. L) and compared their characteristics (Figure 1 and Table 1), in order to clarify the temporal evolution of the magma plumbing system of Towada volcano during the caldera stage.

Harker diagrams (Figure 1) show distinctly different compositional characteristics between ep. N and ep. L. In particular, the range of most trace element compositions from ep. N do not overlap with those of ep. L. As for the compositional trends of incompatible elements in pumices, large ion lithophile element (LILE; e.g., K and Sr) concentrations of ep. L are higher than those of ep. N at the same SiO₂ contents, however high field strength element (HFSE; e.g., Ti and Zr) concentrations of ep. L are lower than those of ep. N. It is possible that the differences of the compositional trends between LILEs and HFSEs originate from the degree of fractionation of amphibole, however it is difficult to explain the compositional gaps of incompatible elements between ep. N and ep. L by AFC of one parental magma. As Yamamoto et al. (2018) pointed out, partial melting of the lower crust of northeast Japan, which contains a large amount of amphiboles (Nishimoto et al., 2005), strongly influences felsic magma generation at Towada volcano. Therefore, differences in HFSE compositions are interpreted to reflect the amount of amphibole released into the melt during partial melting of amphibole-rich lower crust, whereas differences in LILE compositions reflect the degree of overall partial melting of the lower crust. It is assumed that these processes brought about the difference of the compositional trends between LILEs and HFSEs. This suggests that the parental magmas of eruptions ep. N and ep. L are not cogenetic, and that near complete evacuation of the Towada volcano magma chamber during eruption ep. N led to caldera formation and was followed by the recharge, ascent, and evolution of magma derived from an amphibole-rich lower crust prior to ep. L.

Keywords: Towada volcano, The caldera stage, eruptive episode N, eruptive episode L, Northeast Japan

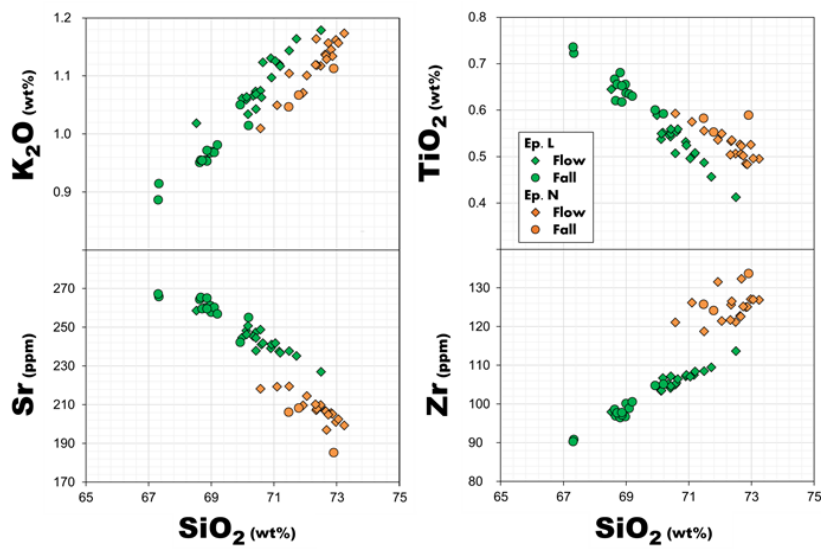


Figure 1 Harker diagrams of selected elements vs. SiO_2

Table 1 Selected compositions of pumices

| | Episode N | | Episode L | |
|-------------------------|-----------|-------|-----------|-------|
| | NK01 | NO13 | LP16 | LF40 |
| (wt%) | | | | |
| SiO_2 | 70.20 | 71.75 | 68.54 | 69.80 |
| TiO_2 | 0.54 | 0.49 | 0.63 | 0.50 |
| Al_2O_3 | 14.16 | 13.59 | 15.35 | 14.59 |
| Fe_2O_3 | 3.33 | 3.03 | 4.01 | 3.09 |
| MnO | 0.12 | 0.12 | 0.14 | 0.12 |
| MgO | 0.82 | 0.69 | 1.07 | 0.79 |
| CaO | 3.15 | 2.97 | 4.28 | 3.71 |
| Na_2O_3 | 4.30 | 4.36 | 4.08 | 4.25 |
| K_2O | 1.04 | 1.14 | 0.96 | 1.10 |
| P_2O_5 | 0.11 | 0.10 | 0.14 | 0.10 |
| Total | 97.77 | 98.22 | 99.19 | 98.04 |
| (ppm) | | | | |
| V | 36.4 | 32.3 | 51.3 | 35.2 |
| Cr | 4.7 | 2.9 | 3.5 | 3.5 |
| Rb | 21.0 | 23.6 | 21.4 | 22.7 |
| Sr | 208.2 | 202.6 | 260.2 | 236.8 |
| Ba | 356.3 | 363.9 | 320.0 | 376.6 |
| Y | 39.9 | 40.0 | 35.9 | 35.2 |
| Zr | 124.1 | 127.0 | 98.9 | 108.4 |
| Nb | 5.3 | 5.1 | 4.6 | 4.9 |